NASA Technical Memorandum 109129

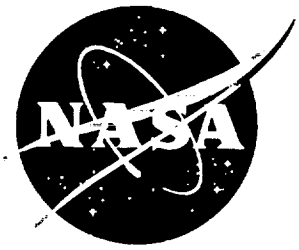

Micromechanical Characterization of Nonlinear Behavior of Advanced Polymer Matrix Composites

T. S. Gates
Langley Research Center, Hampton, Virginia

J. L. Chen and C. T. Sun
Purdue University, West Lafayette, Indiana

June 1994

National Aeronautics and
Space Administration
Langley Research Center
Hampton, Virginia 23681-0001

ABSTRACT: Due to the presence of curing stresses and oriented crystalline structures in th matrix of polymer matrix fiber composites, the in situ nonlinear properties of the matrix ar expected to be rather different from those of the bulk resin. A plane stress micromechanic model was developed to retrieve the in situ elastic-plastic properties of Narmco 5260 and Amoc 8320 matrices from measured elastic-plastic properties of IM7/5260 and IM7/8320 advance composites. In the micromechanical model, the fiber was assumed to be orthotropically elasti and the matrix to be orthotropic in elastic and plastic properties. The results indicate that both i situ elastic and plastic properties of the matrices are orthotropic.

KEY WORDS: micromechanics, polymer matrix composites, temperature, plasticity, off-ax testing.

Introduction

The use of polymer matrix composites (PMC's) in primary and secondary structure is being considered for the High Speed Civil Transport (HSCT) aircraft. This vehicle will be a large commercial transport designed for supersonic flight and a 60,000 hour useful lifetime. It is expected that during supersonic flight, the PMC's will carry high loads under sustained elevated temperature conditions. In such environments, nonlinear and inelastic stress-strain behaviors may become a design concern and therefore must be accounted for in constitutive relations.

For composites consisting of polymer matrices reinforced by high modulus graphite fibers, the inelastic properties of the composite stem from the matrix since the graphite fiber remains basically linearly elastic for the entire temperature range that is of practical interest. Thus, to characterize the nonlinear inelastic properties of the composite, the nonlinear properties of the matrix must be characterized first.

It is assumed that the in situ matrix stress-strain behavior is different from that of the neat resin because of the variation in crystalline structures, the presence of curing stresses, and the interaction between the matrix and the fibers. Thus, the bulk matrix properties cannot be used to represent the matrix properties in the composite. Theoretically, a complete non isothermal inelastic constitutive model could be developed to account for the curing history and to describe the in situ mechanical properties of the matrix. Alternatively, one could retrieve the in situ matrix properties from the measured mechanical properties of the orthotropic plate.

It is conceivable that the amount of work required in the first approach is significantly greater than that of the second approach. Moreover, modeling the orthotropic elastic-plastic and time-dependent elastic-plastic behaviors of fiber composites has been established [1-3]. Simple uniaxial testing of off-axis composite specimens has been shown to be sufficient to characterize these nonlinear properties. In view of the foregoing, the second approach is followed in this study.

To recover the matrix properties from those of the composite, one needs a micromechanical model that predicts composite properties based on matrix properties. Sun and Chen [4] have developed a micromechanical model for composites containing elastic fibers and elastic-plastic matrices. The fiber was assumed to be elastic and orthotropic, and the matrix was assumed to be isotropic. If these constituent properties are known, the global composite elastic-plastic properties can then be calculated.

The present research extends the micromechanical model of [4] to include the in situ orthotropic elastic-plastic properties of the matrix. Using parameters found experimentally in previous studies [5], the off-axis stress-strain curves are produced for two PMC's (IM7/5260 and IM7/8320) under isothermal, elevated temperature test conditions (23°C to 200°C). The micromechanical model is then used to retrieve the in situ matrix properties of these composites.

Micromechanical Model

In the micromechanical model developed by Sun and Chen [4], the composite material is represented by a unit cell containing a fiber of a square cross-section and the surrounding matrix. Inherent in this micromechanical model is the need to know the constituent material properties. Since the in situ matrix properties can be quite different from those of the bulk matrix material, adjustment of the matrix properties in the micromechanical model is often necessary to yield good results [4,6].

The square array of fiber distribution is assumed. To simplify the analysis, the fiber is assumed to have a square cross-section. A quadrant of the representative volume is shown in Fig. 1.

The composite cross-section consists of two major parts, i.e., part A and part B (see Fig. 1). Part B is a pure matrix region, and part A consists of fiber AF and a matrix region denoted by AM. The coordinate system is set up so that the x_1 axis is parallel to the fiber-direction. A state

of plane stress parallel to the x_1–x_2 plane is assumed; i.e., $\sigma_{33} = \sigma_{23} = \sigma_{13} = 0$. In addition, the following assumptions are made:

a. In each subregion, AF, AM, or B, the stress and strain fields are uniform.

b. In region A, the stress fields and strain fields in AF and AM follow the appropriate constant stress or constant strain assumption, i.e.,

$$\sigma_{12}^{AF} = \sigma_{12}^{AM} = \sigma_{12}^{A} \qquad \text{(constant stress)}$$

$$\sigma_{22}^{AF} = \sigma_{22}^{AM} = \sigma_{22}^{A} \qquad \text{(constant stress)} \tag{1}$$

$$\varepsilon_{11}^{AF} = \varepsilon_{11}^{AM} = \varepsilon_{11}^{A} \qquad \text{(constant strain)}$$

c. For the entire micromechanical model, the constant strain assumption is adopted, i.e.,

$$\varepsilon_{11}^{A} = \varepsilon_{11}^{B} = \varepsilon_{11}$$

$$\varepsilon_{22}^{A} = \varepsilon_{22}^{B} = \varepsilon_{22} \tag{2}$$

$$\gamma_{12}^{A} = \gamma_{12}^{B} = \gamma_{12}$$

In equations (1-2), superscripts A, B, AF and AM denote subregions A, B, AF and AM, respectively. For region A that includes subregions AF and AM, the average stresses and strains are

$$\sigma_{ij}^{A} = \frac{1}{AF + AM}\left(\int_{AF} \sigma_{ij}^{AF} dA + \int_{AM} \sigma_{ij}^{AM} dA\right) \tag{3}$$

$$\varepsilon_{ij}^{A} = \frac{1}{AF + AM}\left(\int_{AF} \varepsilon_{ij}^{AF} dA + \int_{AM} \varepsilon_{ij}^{AM} dA\right) \tag{4}$$

For the entire representative volume, the average stresses and strains are

$$\sigma_{ij} = \frac{1}{A + B}\left(\int_{A} \sigma_{ij}^{A} dA + \int_{B} \sigma_{ij}^{B} dA\right) \tag{5}$$

$$\varepsilon_{ij} = \frac{1}{A + B}\left(\int_{A} \varepsilon_{ij}^{A} dA + \int_{B} \varepsilon_{ij}^{B} dA\right) \tag{6}$$

in which A, B, AF and AM denote the areas of designated regions, respectively.

A similar model was proposed by Aboudi [7] who divided the representative volume into four subregions. In each region, a linear variation of displacements was assumed, and the resulting tractions as well as the displacements at the interfaces between the adjacent subregions were required to satisfy the equilibrium and continuity conditions, respectively. Since fewer subregions are considered, the present formulation is somewhat simpler than that of Aboudi.

Substitution of equations (1-2) into equations (3-6) yields

$$\sigma_{11}^{A} = v_1 \sigma_{11}^{AF} + v_2 \sigma_{11}^{AM}$$

$$\varepsilon_{22}^{A} = v_1 \varepsilon_{22}^{AF} + v_2 \varepsilon_{22}^{AM} \tag{7}$$

$$\gamma_{12}^{A} = v_1 \gamma_{12}^{AF} + v_2 \gamma_{12}^{AM}$$

and

$$\sigma_{11} = v_A \sigma_{11}^A + v_B \sigma_{11}^B$$

$$\sigma_{22} = v_A \sigma_{22}^A + v_B \sigma_{22}^B \qquad (8)$$

$$\sigma_{12} = v_A \sigma_{12}^A + v_B \sigma_{12}^B$$

where

$$v_1 = v_A = \frac{h_1}{h_1 + h_2}$$

$$v_2 = v_B = \frac{h_2}{h_1 + h_2}$$

Equations (1-2) and (7-8) are the basic relations between the micromechanical and the corresponding average macromechanical stresses and strains. To establish the relations between the average stresses σ_{ij} and strains ϵ_{ij}, the stress-strain relations of fiber and matrix must be given first.

The fiber is considered an orthotropic linear elastic material. The elastic constants are: E_1^F = longitudinal Young's modulus, E_2^F = transverse Young's modulus, G_{12}^F = in-plane shear modulus, v_{12}^F = Poisson's ratio. Thus, in subregion AF we have the incremental stress-strain relations

$$\{ d\epsilon^F \} = [S^F] \{ d\sigma^F \} \qquad (9)$$

where

$$[S^F] = \begin{bmatrix} \frac{1}{E_1^F} & \frac{-\nu_{21}^F}{E_2^F} & 0 \\ \frac{-\nu_{12}^F}{E_1^F} & \frac{1}{E_2^F} & 0 \\ 0 & 0 & \frac{1}{G_{12}^F} \end{bmatrix} \tag{10}$$

In bulk form, polymer matrices can be considered isotropic. However, inside the composite, the matrix is effectively an anisotropic material. The crystalline structure may become oriented due to the interaction with the fibers and the presence of thermal stresses. Moreover, the actual state of thermal residual stresses in the matrix is quite complicated and cannot be easily predicted. For these reasons, we propose to include all these initial effects in the effective matrix properties.

The matrix material is considered an effectively orthotropic elastic-plastic material for which the plastic strain increments $d\varepsilon_{ij}^{pM}$ are given by

$$d\varepsilon_{ij}^{pM} = d\lambda \frac{\partial J_M}{\partial \sigma_{ij}^M} \tag{11}$$

where $d\lambda$ is a proportionality factor, and the plastic potential J_M is assumed to take the form

$$J_M = \frac{1}{3}\left[r_{11}(\sigma_{11}^M)^2 + (\sigma_{22}^M)^2 + 2r_{12}\sigma_{11}^M\sigma_{22}^M + 2r_{66}(\sigma_{12}^M)^2\right] \tag{12}$$

where r_{11}, r_{12} and r_{66} are coefficients of anisotropy. This is a reduced form for plane stress from the complete quadratic potential for orthotropic materials. Note that for isotropic materials, $r_{11} = 1$, $r_{12} = -0.5$, $r_{66} = 1.5$ and J_M reduces to the classical J_2 function.

Define the effective stress as

$$\bar{\sigma}^M = \sqrt{3J_M} \tag{13}$$

The effective plastic strain increment $d\bar{\varepsilon}^{pM}$ is derived from the plastic work increment,

$$\bar{\sigma}^M d\bar{\varepsilon}^{pM} = \sigma_{ij}^M d\varepsilon_{ij}^{pM} \tag{14}$$

Then,

$$d\bar{\varepsilon}^{pM} = \frac{2}{3} d\lambda \bar{\sigma}^M \tag{15}$$

or

$$d\lambda = \frac{3}{2}\left(\frac{d\bar{\varepsilon}^{pM}}{\bar{\sigma}^M}\right)\left(\frac{d\bar{\sigma}^M}{\bar{\sigma}^M}\right) \tag{16}$$

Using (12) and (16), the explicit plastic stress-strain relations of (11) can be written as

$$\begin{Bmatrix} d\varepsilon_{11}^{pM} \\ d\varepsilon_{22}^{pM} \\ d\gamma_{12}^{pM} \end{Bmatrix} = \frac{1}{H_p}\left(\frac{d\bar{\sigma}^M}{\bar{\sigma}^M}\right) \begin{Bmatrix} r_{11}\sigma_{11}^M + r_{12}\sigma_{22}^M \\ r_{12}\sigma_{11}^M + \sigma_{22}^M \\ 2r_{66}\sigma_{12}^M \end{Bmatrix} \tag{17}$$

where

$$H_p = \frac{d\bar{\sigma}^M}{d\bar{\varepsilon}^{pM}} \tag{18}$$

is called the generalized plastic modulus of the matrix material, which, in general, is a function of the loading history.

Rewriting equation (17) in matrix form in terms of stress increments and adding to it the elastic strain components, we obtain

$$\{ d\varepsilon^M \} = [S^M] \{ d\sigma^M \} \tag{20}$$

where

$$\{ d\varepsilon^M \} = \begin{Bmatrix} d\varepsilon_{11}^M \\ d\varepsilon_{22}^M \\ d\gamma_{12}^M \end{Bmatrix} \quad , \quad \{ d\sigma^M \} = \begin{Bmatrix} d\sigma_{11}^M \\ d\sigma_{22}^M \\ d\sigma_{12}^M \end{Bmatrix} \tag{21}$$

$[S^M]$ is the elastic-plastic compliance matrix whose entities are given by

$$S_{11}^M = \frac{1}{E_1^M} + \Omega^M (r_{11}\sigma_{11}^M + r_{12}\sigma_{22}^M)^2$$

$$S_{12}^M = \frac{-\nu 21^M}{E_2^M} + \Omega^M (r_{11}\sigma_{11}^M + r_{12}\sigma_{22}^M)(r_{12}\sigma_{11}^M + \sigma_{22}^M)$$

$$S_{16}^M = \Omega^M \, 2r_{66}\sigma_{12}^M (r_{11}\sigma_{11}^M + r_{12}\sigma_{22}^M)$$

$$S_{21}^M = S_{12}^M \tag{22}$$

$$S_{22}^M = \frac{1}{E_2^M} + \Omega^M (r_{12}\sigma_{11}^M + \sigma_{22}^M)^2$$

$$S_{26}^M = \Omega^M 2r_{66}(r_{12}\sigma_{11}^M + \sigma_{22}^M)$$

$$S_{61}^{M} = S_{16}^{M}$$

$$S_{62}^{M} = S_{26}^{M}$$

$$S_{66}^{M} = \frac{1}{G_{12}^{M}} + \Omega^{M}(2r_{66}\sigma_{12}^{M})^2$$

where

$$\Omega^{M} = \frac{1}{H_p}\,\frac{1}{(\bar{\sigma}^{M})^2}$$

Applying the matrix model mentioned above to Part AM, we obtain

$$\{ d\varepsilon^{AM} \} = [S^{AM}] \{ d\sigma^{AM} \} \tag{23}$$

in which the compliances S_{ij}^{AM} depend on the elastic and plastic properties of the matrix. Equations (1), (9) and (23) are used to eliminate σ_{ij}^{AF}, σ_{ij}^{AM}, ε_{ij}^{AF}, and ε_{ij}^{AM} in equation (7) with the result

$$\begin{Bmatrix} d\varepsilon_{11}^{A} \\ d\varepsilon_{22}^{A} \\ d\gamma_{12}^{A} \end{Bmatrix} = \begin{bmatrix} S_{11}^{A} & S_{12}^{A} & S_{16}^{A} \\ S_{21}^{A} & S_{22}^{A} & S_{26}^{A} \\ S_{61}^{A} & S_{62}^{A} & S_{66}^{A} \end{bmatrix} \begin{Bmatrix} d\sigma_{11}^{A} \\ d\sigma_{22}^{A} \\ d\sigma_{12}^{A} \end{Bmatrix} \tag{24}$$

Inverting equation (24), we obtain

$$\{ d\sigma^{A} \} = [C^{A}] \{ d\varepsilon^{A} \} \tag{25}$$

Region B contains only the matrix. The incremental stress-strain relations are given by

$$\{ d\varepsilon^B \} = [S^B] \{ d\sigma^B \} \tag{26}$$

where S_{ij}^B are identical to S_{ij}^{AM}.

Inverting equation (26), we obtain

$$\{ d\sigma^B \} = [C^B] \{ d\varepsilon^B \} \tag{27}$$

where

$$[C^B] = [S^B]^{-1} \tag{28}$$

From equation (8) together with equations (25) and (27), we obtain the incremental stress-strain relation for the composite,

$$\{ d\sigma \} = [C] \{ d\varepsilon \} \tag{29}$$

where

$$[C] = v_A [C^A] + v_B [C^B] \tag{30}$$

The inverse relation of equation (29) is

$$\{d\varepsilon\} = [S]\{d\sigma\} \tag{31}$$

where

$$[S] = [C]^{-1} \tag{32}$$

In Situ Elastic-Plastic Matrix Properties

The incremental stress-strain relations given by equation (31) are nonlinear since S_{ij} depend on the current state of stress in the matrix, i.e., σ_{ij}^{AM} and σ_{ij}^B. An incremental numerical

procedure can be used to obtain the solution.

The incremental stress-strain relations given by equation (31) can be used to predict the elastic-plastic stress-strain behavior of composites if the in situ fiber and matrix properties are known. Conversely, these relations can be used to estimate the in situ matrix properties based on the composite stress-strain data.

Although neat resins are usually considered isotropic materials, the in situ resin matrix elastic and plastic properties may not be isotropic. This is due to the presence of thermal residual stresses in the composite and oriented crystalline structures in the matrix caused by thermal stresses during curing. For this reason, we then assume that the matrix is elastically orthotropic and its initial plastic behavior is also orthotropic. In plane stress, four elastic constants E_1^M, E_2^M, G_{12}^M and ν_{12}^M are to be determined. Three orthotropy coefficients in the plastic potential (see equation (12)), r_{11}, r_{12} and r_{66} are needed. In addition, the effective stress-effective plastic strain relation must be determined. In this study, the power law is employed, i.e.,

$$\bar{\varepsilon}^{pM} = \beta (\bar{\sigma}^{M})^{\alpha} \tag{33}$$

where α and β are two temperature-dependent coefficients.

The composite elastic-plastic stress-strain behavior can be described by its off-axis stress-strain curves [1]. For an off-axis coupon specimen under a uniaxial stress σ_x the total strain is obtained as [1]

$$\varepsilon_x = \frac{\sigma_x}{E_x} + h(\theta)^{n+1} K(\sigma_x)^n \tag{34}$$

where E_x is the apparent elastic modulus in the loading (x-) direction, K and n are material constants, and

$$h(\theta) = [\frac{3}{2}(\sin^4\theta + 2a_{66}\sin^2\theta\cos^2\theta)]^{1/2} \tag{35}$$

In equation (35), θ is the off-axis angle and a_{66} is the orthotropy coefficient describing the orthotropic nature of initial plasticity of the composite.

The first term on the right-hand-side of equation (34) represents the elastic part of the strain, and the second term represents the plastic strain. From the coordinate transformation law, the apparent modulus E_x can be calculated from the principal elastic moduli E_1, E_2, G_{12} and ν_{12} as

$$\frac{1}{E_x} = \frac{\cos^4\theta}{E_1} + (\frac{1}{G_{12}} - 2\frac{\nu_{12}}{E_1})\sin^2\theta\cos^2\theta + \frac{\sin^4\theta}{E_2} \tag{36}$$

The second term on the right-hand-side of equation (34) represents the plastic strain. For fiber composites, the plastic strain increments can be derived from the flow rule similar to that of equation (11) with the one-parameter plastic potential [1],

$$J_{comp} = \frac{1}{2}(\sigma_{22}^2 + a_{66}\sigma_{12}^2) \tag{37}$$

together with the effective stress-effective plastic strain relation

$$\bar{\varepsilon}^p = K(\bar{\sigma})^n \tag{38}$$

where

$$\bar{\sigma} = \sqrt{3J_{comp}}$$

Materials and Specimens

Two advanced PMC's were selected for this study. The first, IM7/8320, is a graphite/thermoplastic manufactured by AMOCO Corporation and fabricated in a hot press at NASA Langley Research Center (LaRC). The second PMC, IM7/5260, a graphite/bismaleimide, was manufactured by BASF Corporation and autoclave fabricated at NASA LaRC. The glass transition temperatures, T_g, of the manufactured panels were measured by DSC at NASA LaRC to be 220°C and 240°C for the IM7/8320 and IM7/5260, respectively.

All panels were C-scanned prior to cutting the specimens and inspected for visible defects. Tensile test specimens cut from the panels measured 241 mm x 25 mm and were 12 plies thick. Longitudinal and transverse elastic constants were measured from [0] to [90] layups, respectively. The shear modulus was measured from a $[\pm 45]_{3s}$ layup.

Composite Material Testing

Specific explanations of the test methods used to obtain the material constants for the orthotropic plate can be found in [8]. Testing was performed with a servo-hydraulic test machine capable of running predetermined load or strain history profiles. Load, as measured by the load cell, was converted to stress using the average cross sectional area of the specimen measured prior to testing. Axial strain was measured on the off-axis tests by using extensometers. Two extensometers, mounted opposite each other, were placed along the specimen's thin edge in the center section. For the $[0]_{12}$ and $[\pm 45]_{2s}$ specimens, which required both axial and transverse strain measurement, back-to-back, center mounted strain gages were used.

In addition to the elastic constants, only three material constants are required for the orthotropic plasticity model for any given temperature. These constants are: a_{66} for the plastic potential function and K and n for the quasistatic plastic stress-strain relations. These constants

were all found using data from simple off-axis tension tests. By testing under strain control, all of the constants were extracted from uniaxial tests with repeated hold times built in to allow for stress relaxation. During stress relaxation, the stress decreased rapidly towards some limiting value. This limiting value was assumed to be the quasistatic stress and represented the stress needed to solve the elastic/plastic quasistatic equation for a given strain. By repeating these periods of stress relaxation during the course of the test, enough quasistatic points were obtained to allow a smooth curve to be constructed to represent the quasistatic behavior.

Once the quasistatic points were known, a smooth stress/strain curve was then generated through these points and converted into an effective stress-effective plastic strain curve. These uniaxial stress-plastic strain curves from different off-axis tests were then plotted together and collapsed into a single master curve by selecting the appropriate value of a_{66}. The master curve was then fit with a power law relation which defined the values of K and n (see equation (34)) needed by the quasistatic analysis.

Results

The orthotropic elastic-plastic properties of IM7/5260 and IM7/8320 composites have been obtained by Gates [5] using off-axis coupons specimens. In Table 1 the elastic moduli E_1, E_2, G_{12}, ν_{12} and coefficients K, n, a_{66}, in the plasticity models for the two composites are reproduced from [5]. These composite properties are used to recover the in situ matrix properties.

Since there are a number of constants to be determined based on the composite data, it is necessary to start by using some fiber and matrix properties that we are relatively certain of. For instance, carbon fiber IM7 is a temperature-stable linearly elastic material whose longitudinal modulus E_1^F and Poisson's ratio ν_{12}^F have been reported. Usually, the fiber volume fraction of the composite is determined by other methods. Starting with this initial information, we then proceed to match the measured composite elastic moduli with those predicted by the

micromechanical model.

From the 0^o and 90^o specimens, E_1, E_2 and ν_{12} of the composite are directly determined. Since the longitudinal property of the 0^o specimen is strongly dominated by the longitudinal modulus E_1^F of the fiber, this data can be used to check the value of E_1^F and the fiber volume fraction. From the micromechanical model and the 0^o and 90^o composite data, we obtain E_2^F, E_1^M, E_2^M and ν_{12}^M. From other off-axis specimen data, G_{12}^F and G_{12}^M are determined. Of course, this procedure is iterative, and these unknown elastic constants can be varied to fit all the composite data.

After the elastic constants are determined, we then proceed to determine the coefficients in the plasticity model for the matrix using the entire stress-strain curves of the composite. The coefficients to be determined are r_{11}, r_{12}, r_{66}, β and α.

Based on our experience, in a fiber composite, the index α of the power law, equation (33), for the matrix is similar to that (n) of the composite (see equation (34)). Thus, we set $\alpha = n$. The numerical results also indicate that $r_{11} = 1$ and $r_{12} = -0.5$ which are the same as in the J_2 function of isotropic materials. This is consistent with the result for matrix elastic moduli, i.e., $E_1^M = E_2^M$. Therefore, only two coefficients r_{66} and β must be determined.

The fiber volume fraction is found to be 0.55 for both composites. The elastic moduli of the IM7 carbon fiber are

$$E_1^F = 276.0 \text{ GPa} \quad , \quad E_2^F = 13.8 \text{ GPa} \quad , \quad \nu_{12}^F = 0.25 \quad , \quad G_{12}^F = 20.0 \text{ GPa}$$

The results for the elastic and plastic properties of Narmco 5260 and Amoco 8320 are listed in Tables 2 and 3, respectively.

Discussion

From the results listed in Tables 2 and 3, we see that the orthotropy coefficient r_{66} remains almost constant over the entire temperature range. For isotropic materials, $r_{66} = 1.5$. Thus, we can say that Amoco 8320 is plastically more anisotropic than Narmco 5260. The greater in situ matrix plastic orthotropy of both matrices implies the presence of significant effects of thermal residual stresses in the composites.

It is interesting to compare the values of α for the two matrix systems. For Narmco 5260, the value of α increases as temperature increases. This implies that at lower temperatures, the matrix exhibits greater hardening, and that at higher temperatures, the matrix approaches an ideal elastic-perfectly plastic solid. On the other hand, the value of α for Amoco 8320 decreases toward the region of high temperatures. This indicates that at high temperatures either the matrix hardens plastically or it fails at small strains before plasticity is fully displayed.

Figure 2 presents the representative effective stress-effective plastic strain curves (the master curves) for IM7/5260 at 175°C and 150°C obtained by Gates [5]. Figure 3 shows the total stress-strain curves for IM7/5260 for a number of off-axis specimens derived from the master curve given in Fig. 2. Using the recovered in situ matrix properties together with the fiber elastic moduli, the stress-strain curves for the off-axis specimens are calculated for both composite systems at various temperatures. The results are presented in Figs. 4-15 along with some of the original data from individual specimens.

Comparison of the predicted and measured behavior, as shown in Figs. 4-15, indicates that the micromechanical model can describe the off-axis stress-strain curves through the use of the recovered in situ matrix properties. These figures show a good comparison for a number of off-axis angles covering a wide range of test temperatures. Only the data for the 25° specimen of IM7/8320 at 120°C (Fig. 6) shows a poor correlation between test and prediction.

Examination of Figs. 4-15 leads to some general comments regarding the accuracy of the model and the reliability of the test data. First, it should be noted that the predictions were made out to approximately 2% strain; however, the test data typically ended prior to 1% strain levels. It is recognized that prediction beyond the range of test data is purely extrapolation and remains to be verified. Most of the specimens tested had off-axis angles from 15° to 30°. Off-axis tests in this angle range will experience the highest degree of extension-shear coupling. This coupling, which is known to cause bending stress across the width of the specimen may be a source of error when measuring axial strains.

Although the test data given in the figures represent averaged values of repeated tests, most of the predicted curves lay below the test data. This may be due to the fact that the elastic-plastic stress-strain response was measured by performing multiple stress relaxation events during the course of a strain controlled test [8]. Since a "true" time-independent response is not experimentally obtainable, the elastic-plastic data represent the quasistatic behavior.

Another source of possible error may occur in the procedure of estimating the shear modulus G_{12}^F of the fiber. It was found that the composite properties were not sensitive to the variation of G_{12}^F. The value of G_{12}^F chosen for this study may not have been accurate. It would be highly advantageous to determine the fiber elastic constants separately since the fiber properties are not altered in the composite.

Conclusion

A micromechanical model consisting of an elastic fiber and an orthotropic elastic-plastic matrix has been developed to predict composite elastic-plastic behavior. It was demonstrated that this model can be used to retrieve the in situ elastic and plastic matrix properties from the composite properties. Due to the presence of unknown thermal residual stresses and oriented crystalline structures, the matrix should be assumed to be effectively orthotropic in elastic and plastic properties. The predicted off-axis tensile stress-strain behavior compares favorably to the

measured response of the two advanced PMC's at elevated temperatures.

Acknowledgement -- The work performed at Purdue University was supported by a NASA Research Center Grant No. NAG-1-1366 to Purdue University.

References

[1] Sun, C. T., and Chen, J. L., "A Simple Flow Rule for Characterizing Nonlinear Behavior of Fiber Composites," *Journal of Composite Materials,* Vol. 23, No. 10, 1989, pp. 1009-1020.

[2] Chen, J. L., and Sun, C. T., "A Plastic Potential Function Suitable for Anisotropic Fiber Composites," *Journal of Composite Materials,* Vol. 27, No. 14, 1993, pp. 1379-1390.

[3] Gates, T. S., and Sun, C. T., "An Elastic/Viscoplastic Constitutive Model for Fiber Reinforced Thermoplastic Composites," *AIAA Journal,* Vol. 29, No. 3, 1991, pp. 457-463.

[4] Sun, C. T. and Chen, J. L., "A Micromechanical Model for Plastic Behavior of Fibrous Composites," *Composites Science & Technology,* Vol. 40, No. 2, 1991, pp. 115-129.

[5] Gates, T. S., "Rate Dependent Stress-Strain Behavior of Advanced Polymer Matrix Composites," *NASA Technical Memorandum 104070,* NASA Langley Research Center, April 1991.

[6] Bahei-El-Din, Y. A., and Dvorak, G. J., "Plastic Deformation of a Laminated Plate with a Hole," *Journal of Applied Mechanics,* Vol. 47, 1980, pp. 827-832.

[7] Aboudi, J., *Mechanics of Composite Materials, A Unified Mechanical Approach,* Elsevier, New York, NY, 1991.

[8] Gates, T. S., "Experimental Characterization of Nonlinear, Rate Dependent Behavior in Advanced Polymer Matrix Composites," *Experimental Mechanics,* Vol. 32, No. 1, March 1992, pp. 68-73.

Table 1--Tensile Elastic and Plastic Properties of IM7/5260 and IM7/8320 Composites [5].

Material		Elastic					Elastic/Plastic	
Type	°C	E_1 (GPa)	E_2 (GPa)	G_{12} (GPa)	ν_{12}	a_{66}	K(MPa)$^{-n}$	n
	23	152.8	8.7	5.2	0.30	0.60	5.07E-10	3.34
IM7/5260	70	161.7	9.2	5.7	0.31	0.60	1.13E-09	3.35
Tension	125	156.5	8.8	5.3	0.36	0.60	1.18E-09	3.63
	150	165.3	8.8	5.1	0.35	0.60	8.74E-12	4.96
	175	136.4	7.7	5.1	0.30	0.60	1.74E-14	7.06
	200	154.3	7.5	5.1	0.35	0.60	2.17E-17	9.64
	23	157.9	7.1	4.3	0.32	0.30	8.86E-12	5.48
IM7/8320	70	153.8	7.9	4.3	0.34	0.30	2.19E-08	3.36
Tension	125	142.0	7.5	4.7	0.35	0.30	3.61E-11	5.50
	150	152.9	7.3	4.4	0.33	0.30	2.48E-12	6.28
	175	153.9	7.2	3.4	0.32	0.30	4.85E-08	3.84
	200	147.3	5.5	2.6	0.35	0.30	6.16E-05	2.66

Table 2. Predicted Properties for Matrix Narmco 5260

Temp.(°C)	23	70	125	150	175	200
E_1(GPa)	4.69	4.69	4.69	4.69	3.81	3.65
E_2(GPa)	4.69	4.69	4.69	4.69	3.81	3.65
G_{12}(GPa)	1.70	1.70	1.70	1.70	1.68	1.68
ν_{12}	0.38	0.38	0.38	0.38	0.38	0.38
r_{66}	0.56	0.55	0.58	0.54	0.53	0.53
$\beta(MPa)^{-\alpha}$	$0.35X10^{-8}$	$0.76X10^{-8}$	$0.91X10^{-8}$	$0.1X10^{-9}$	$0.38X10^{-12}$	$0.1X10^{-14}$
α	3.34	3.35	3.63	4.96	7.06	9.64

Table 3. Predicted Properties for Matrix Amoco 8320

Temp.(°C)	23	70	125	150	175	200
E_1(GPa)	3.40	3.40	3.40	3.40	3.32	2.20
E_2(GPa)	1.90	3.40	3.40	3.40	3.32	2.20
G_{12}(GPa)	1.44	1.44	1.44	1.35	1.12	.85
ν_{12}	0.4	0.4	0.4	0.4	0.4	0.4
r_{66}	0.28	0.28	0.28	0.25	0.3	0.3
$\beta(MPa)^{-\alpha}$	$0.12X10^{-3}$	$0.17X10^{-6}$	$0.5X10^{-9}$	$0.29X10^{-8}$	0.410^{-6}	$0.36X10^{-3}$
α	5.48	3.36	5.48	6.28	3.84	2.66

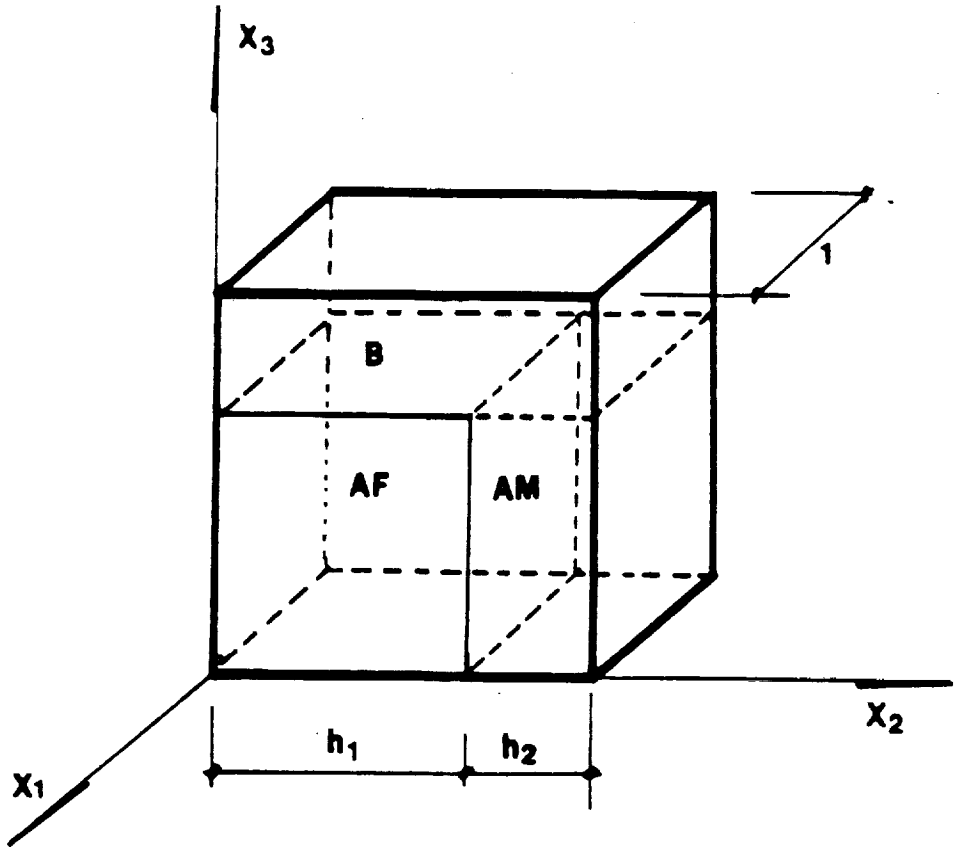

Fig. 1--Geometry of the micromechanical model.

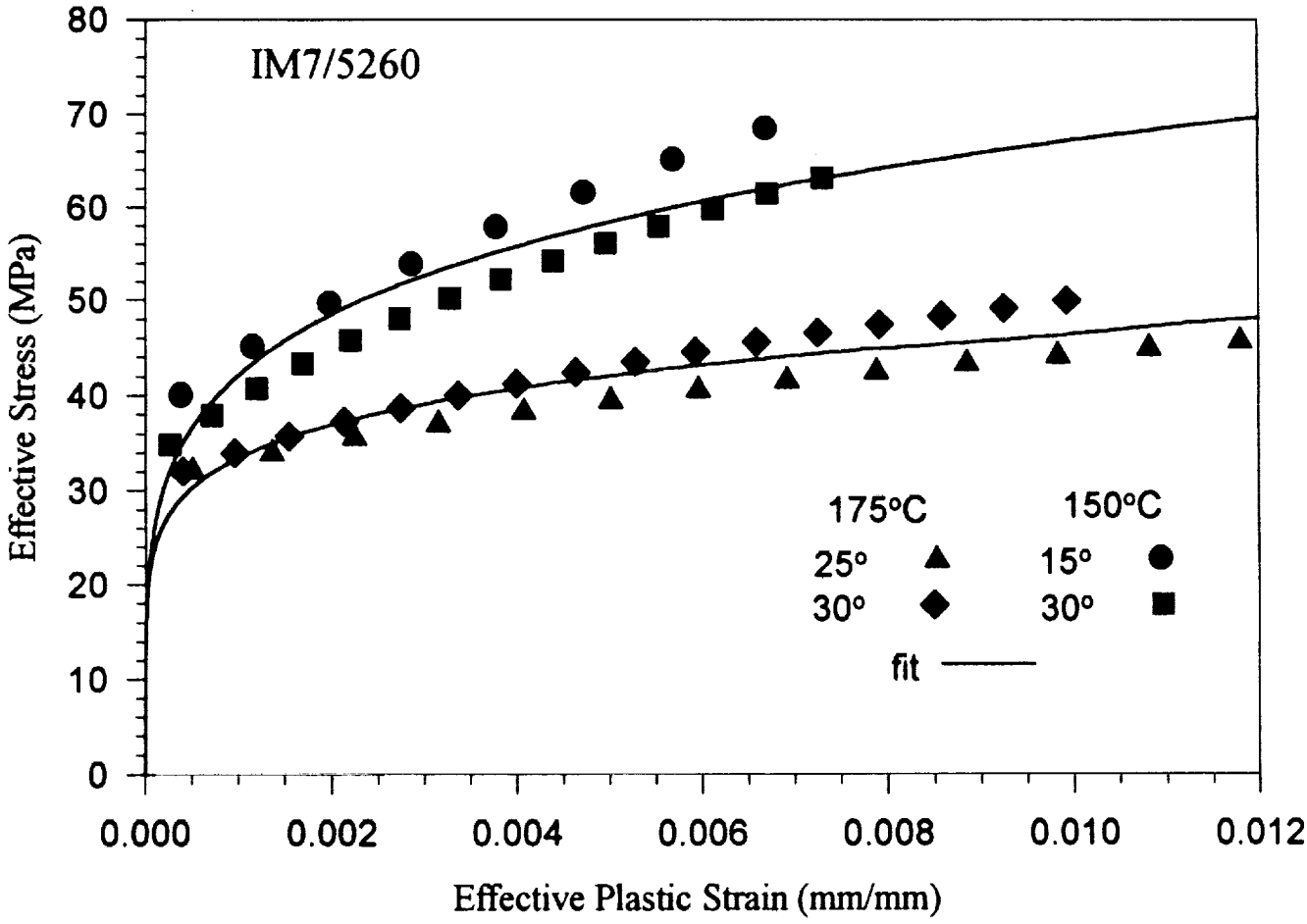

Fig. 2--Representative master curves and data for IM7/5260.

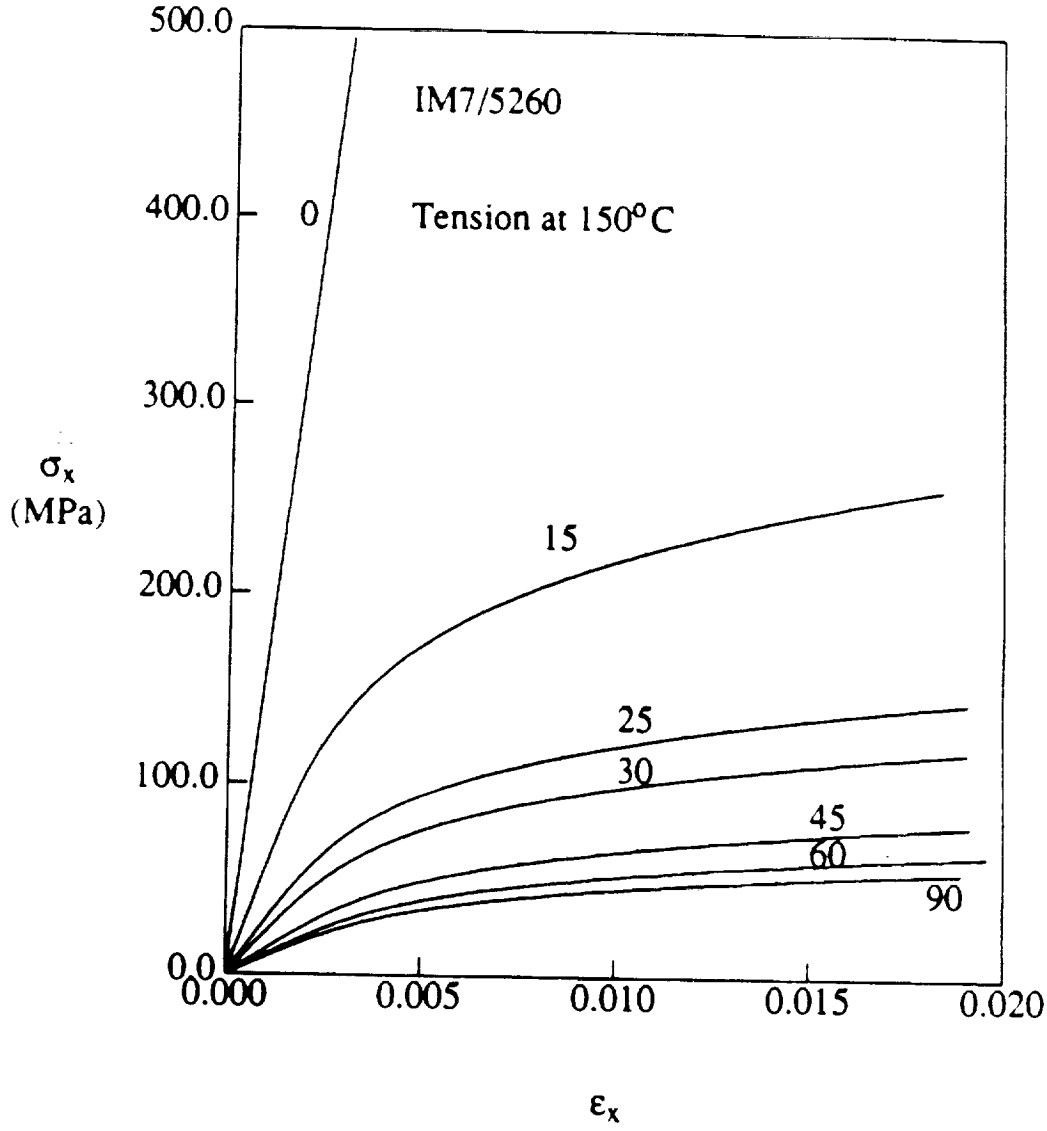

Fig. 3 Quasi-static tensile stress-strain curves for IM7/5260 at 150° C (the label to each curve indicates off-axis angle)

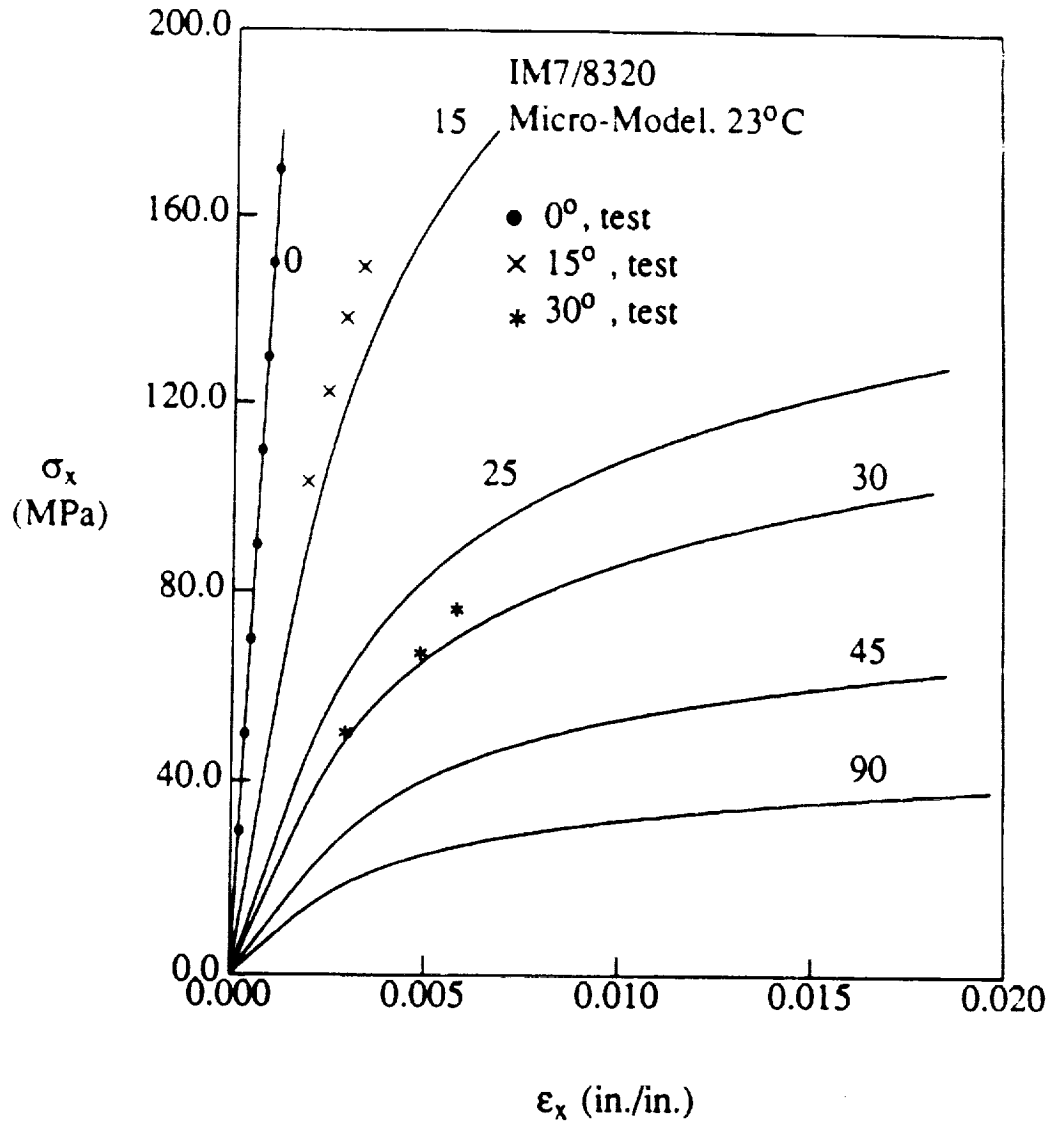

Fig. 4 Stress-strain curves for IM7/8320 at 23° C predicted by the micromechanical model. Symbols represent data from individual specimens.

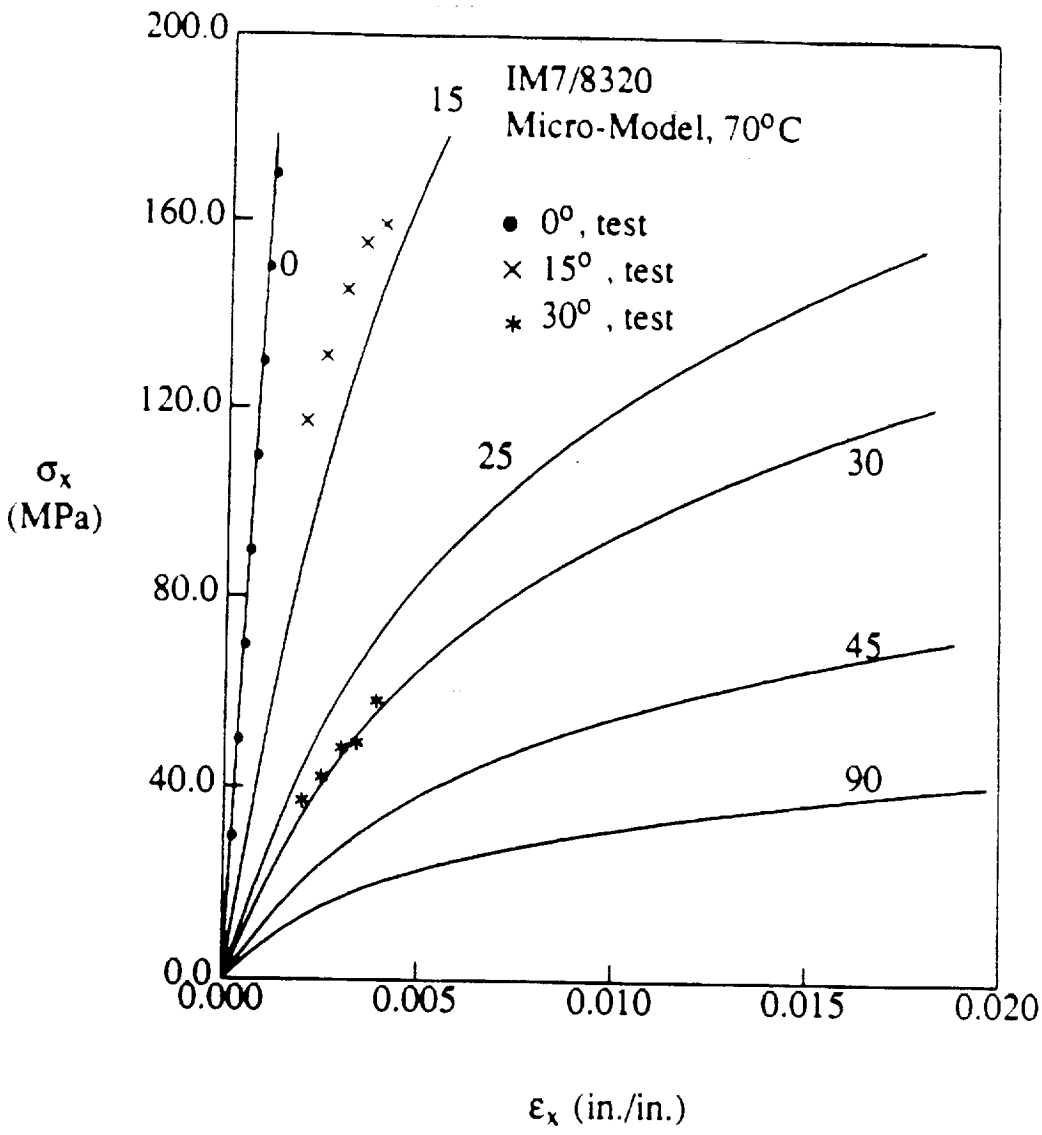

Fig. 5 Stress-strain curves for IM7/8320 at 70° C predicted by the micromechanical model. Symbols represent data from individual specimens.

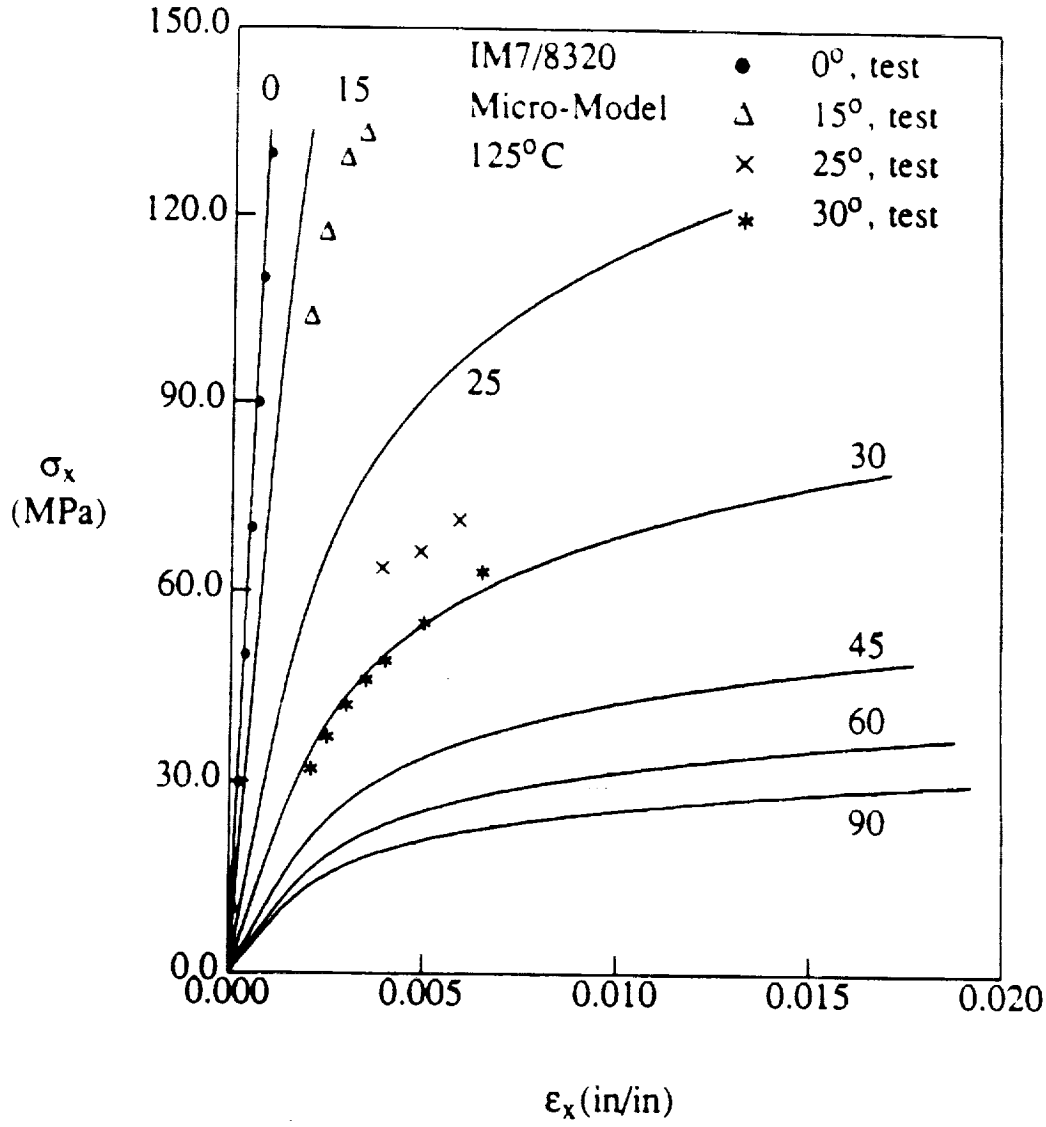

Fig. 6 Stress-strain curves for IM7/8320 at 125° C predicted by the micromechanical model. Symbols represent data from individual specimens.

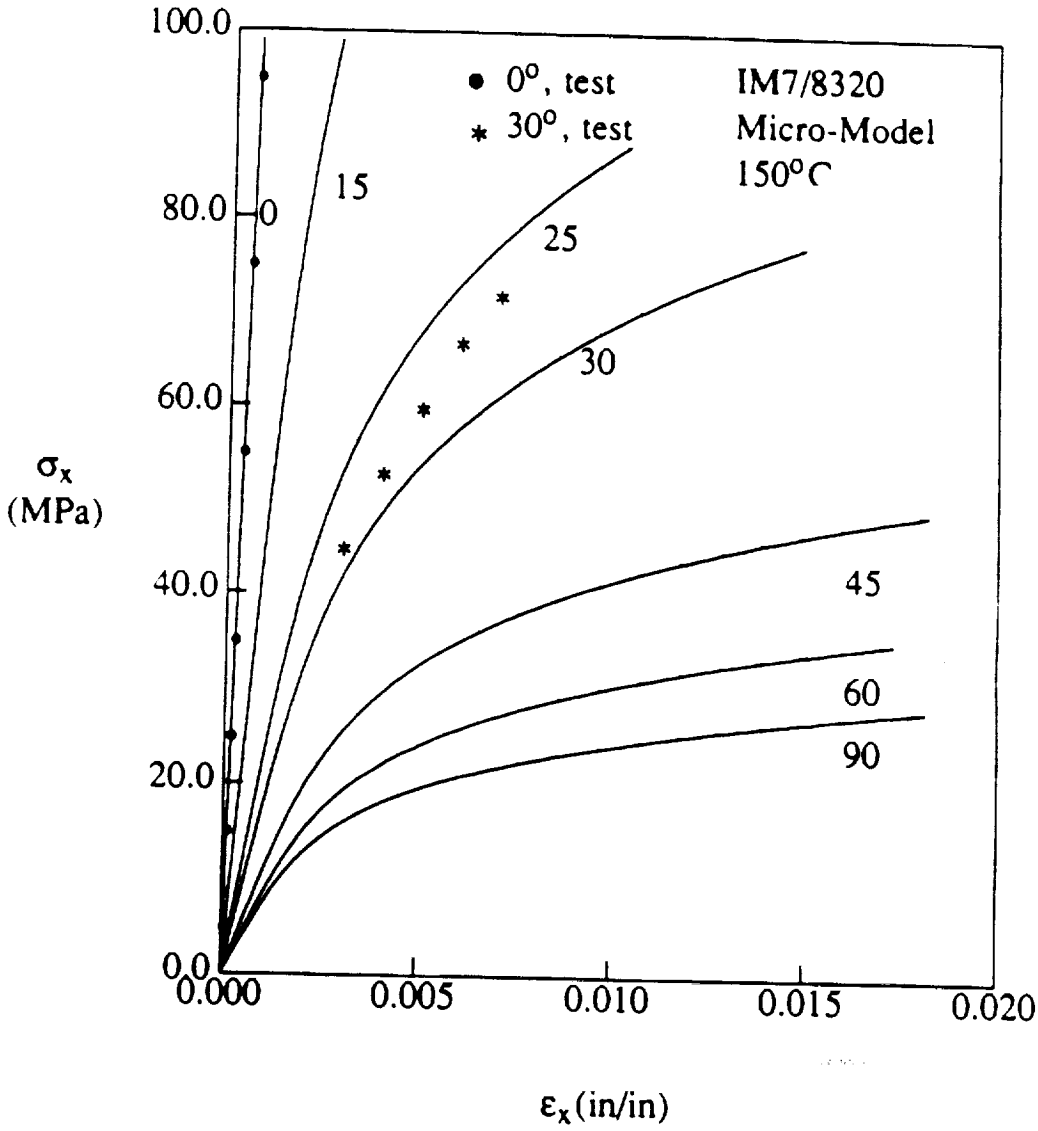

Fig. 7 Stress-strain curves for IM7/8320 at 150° C predicted by the micromechanical model. Symbols represent data from individual specimens.

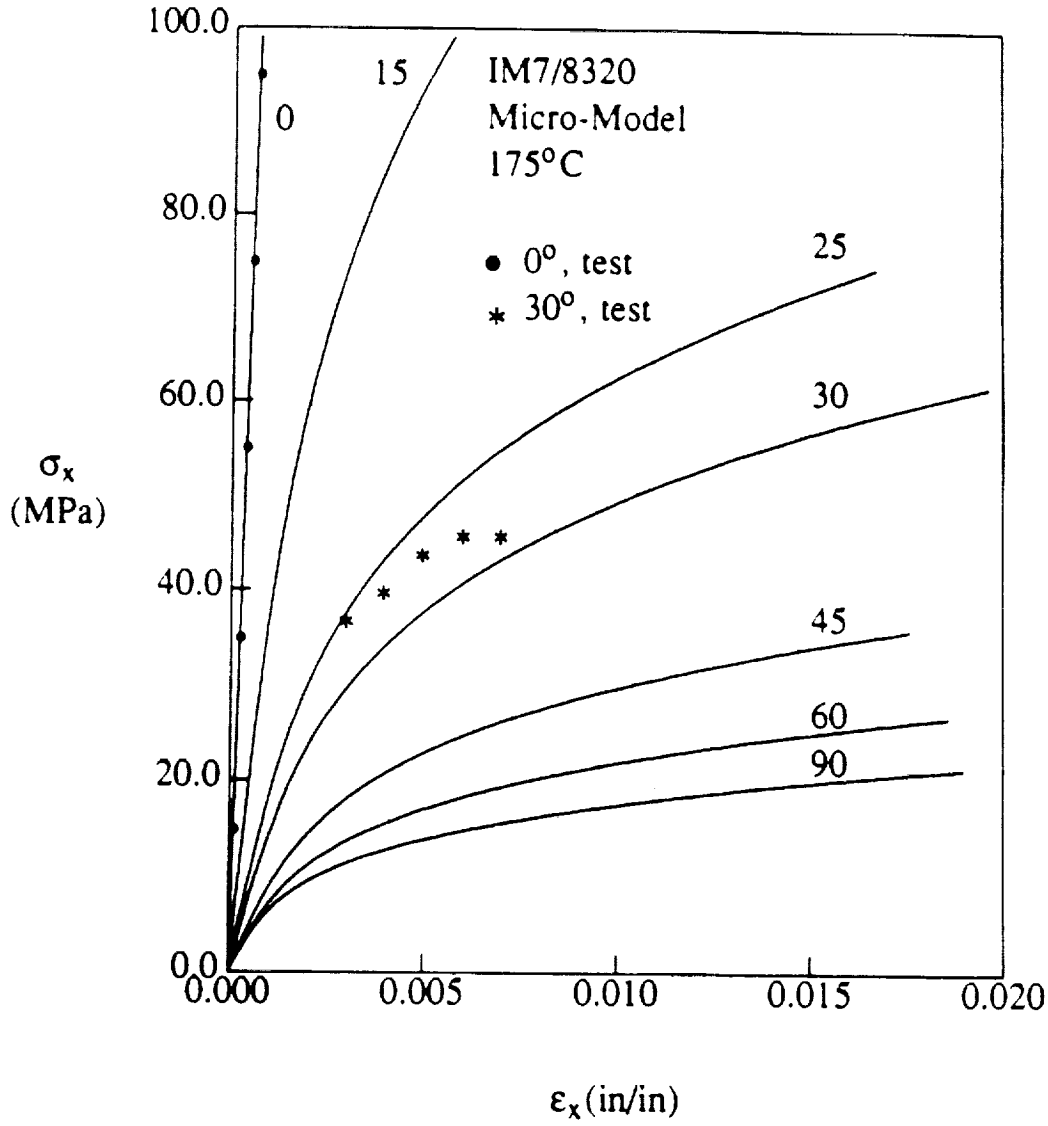

Fig. 8 Stress-strain curves for IM7/8320 at 175° C predicted by the micromechanical model. Symbols represent data from individual specimens.

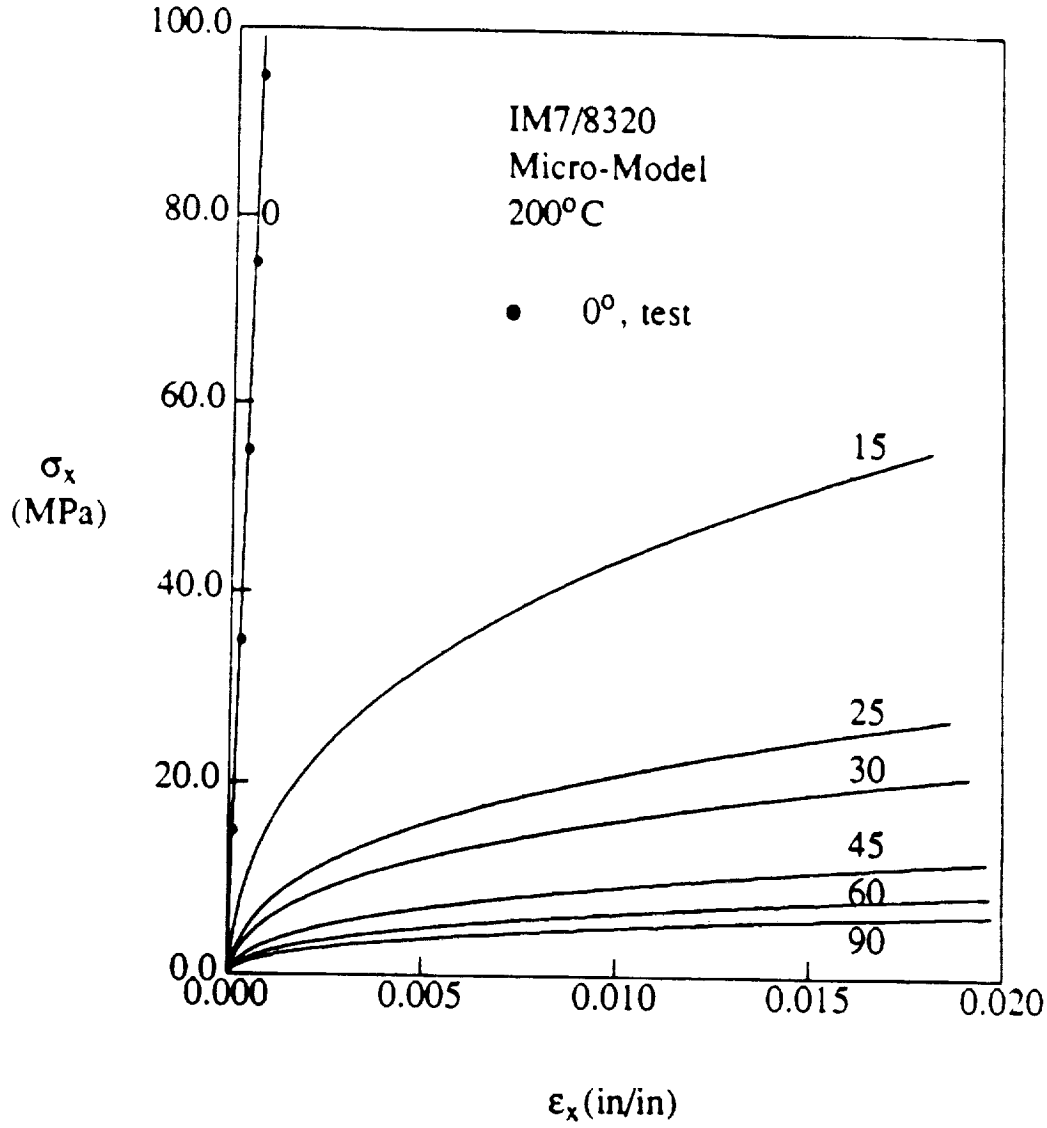

Fig. 9 Stress-strain curves for IM7/8320 at 200° C predicted by the micromechanical model. Symbols represent data from individual specimens.

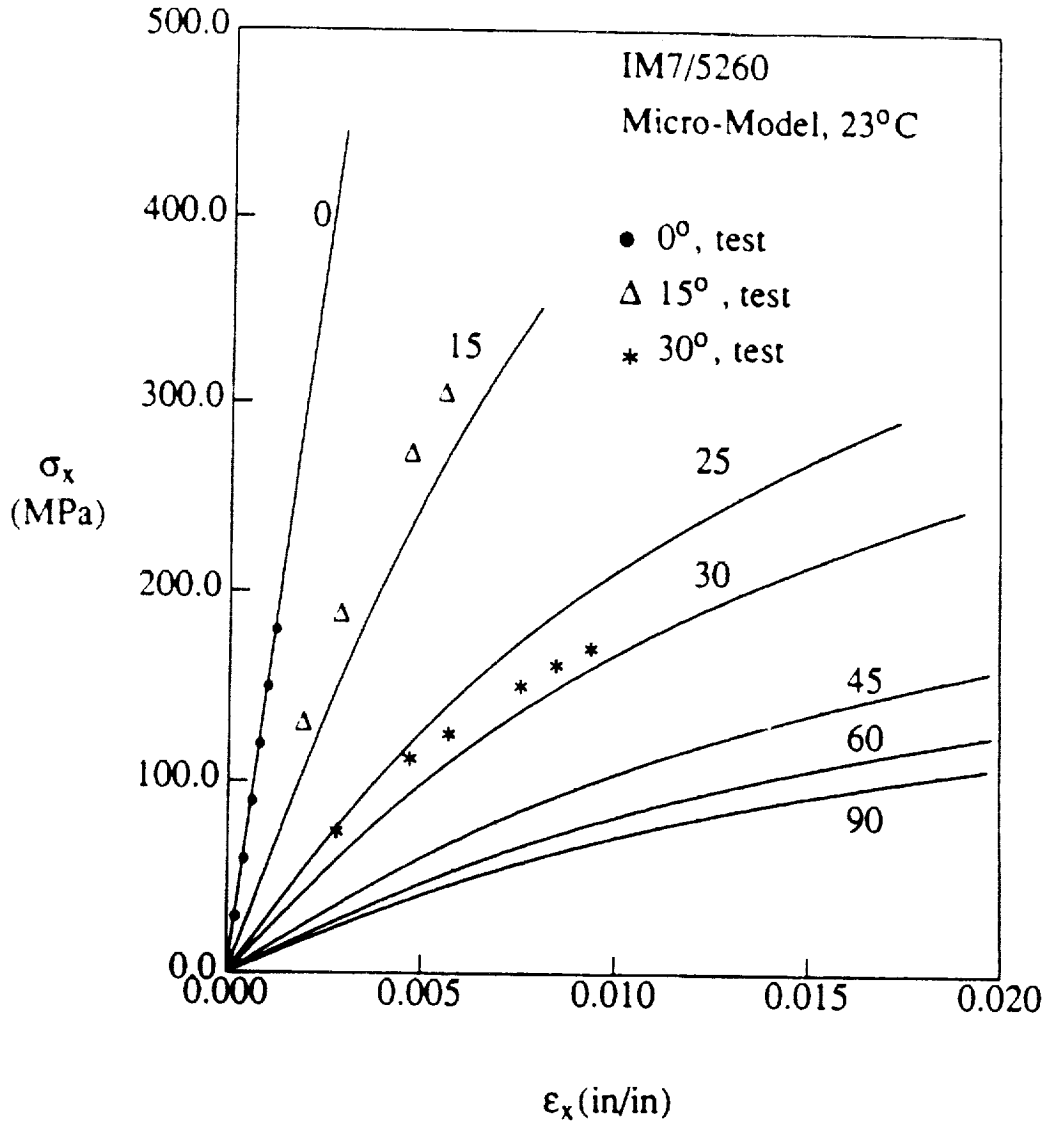

Fig. 10 Stress-strain curves for IM7/5260 at 23° C predicted by the micromechanical model. Symbols represent data from individual specimens.

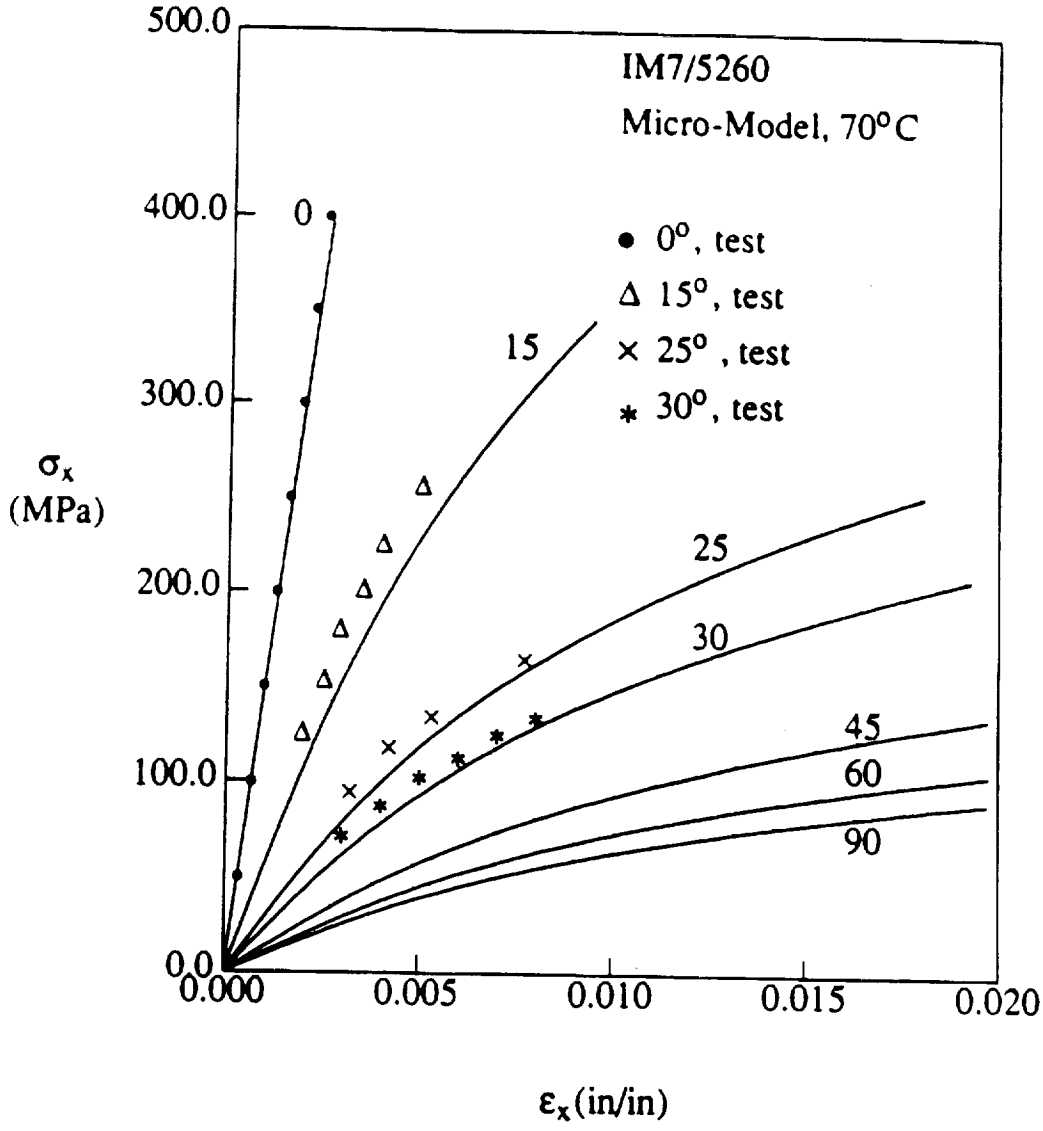

Fig. 11 Stress-strain curves for IM7/5260 at 70° C predicted by the micromechanical model. Symbols represent data from individual specimens.

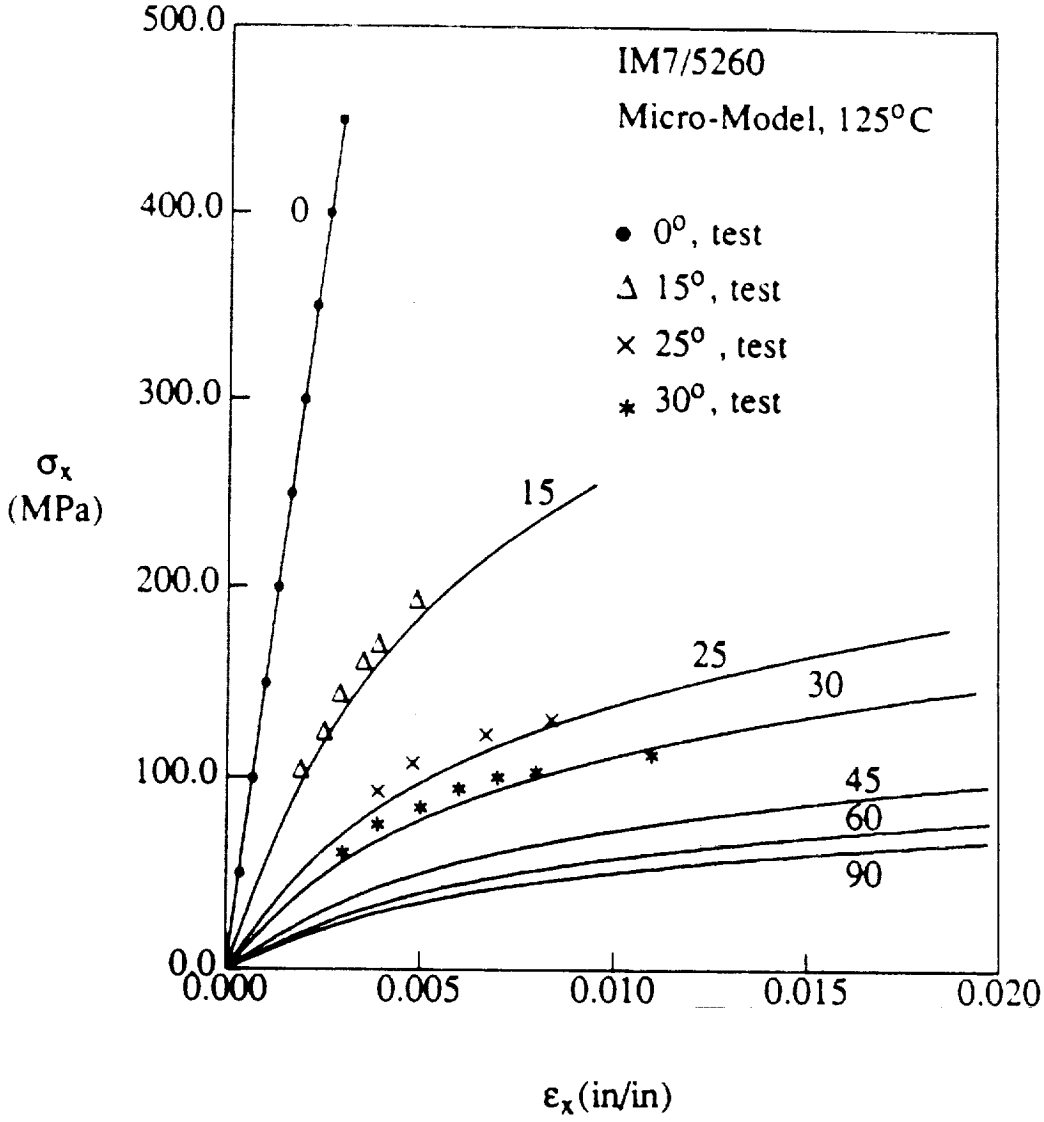

Fig. 12 Stress-strain curves for IM7/5260 at 125° C predicted by the micromechanical model. Symbols represent data from individual specimens.

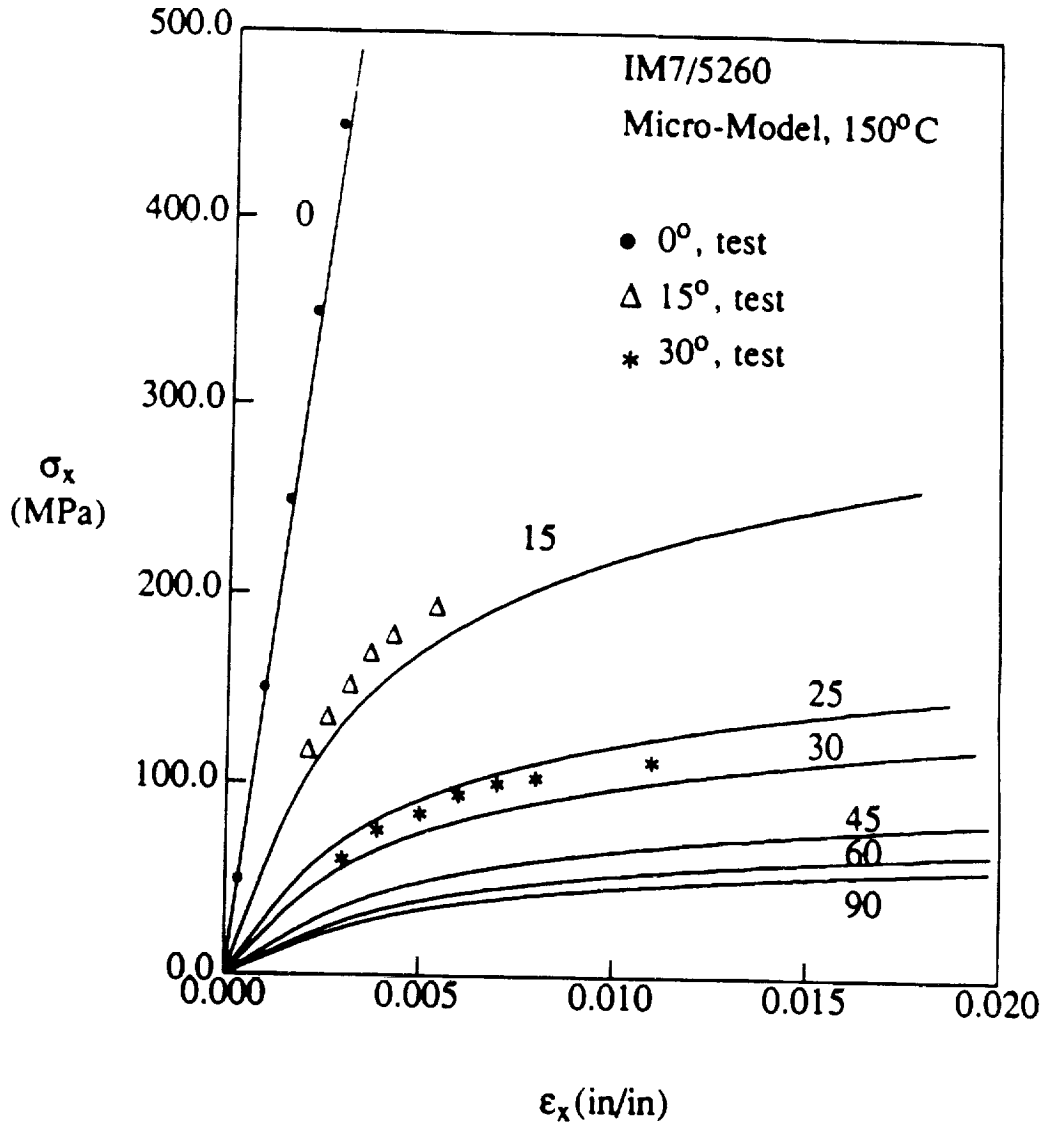

Fig. 13 Stress-strain curves for IM7/5260 at 150° C predicted by the micromechanical model. Symbols represent data from individual specimens.

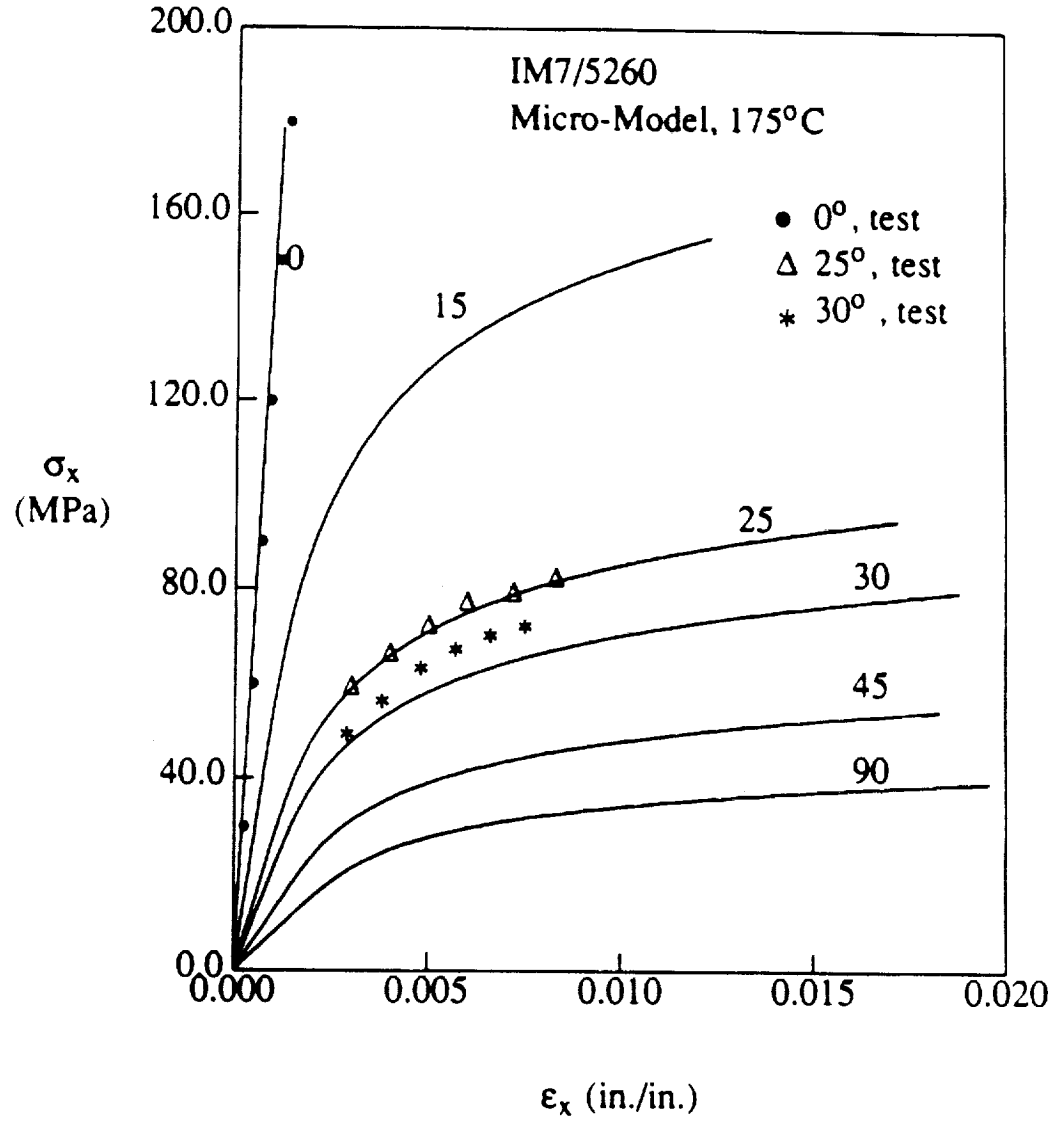

Fig. 14 Stress-strain curves for IM7/5260 at 175° C predicted by the micromechanical model. Symbols represent data from individual specimens.

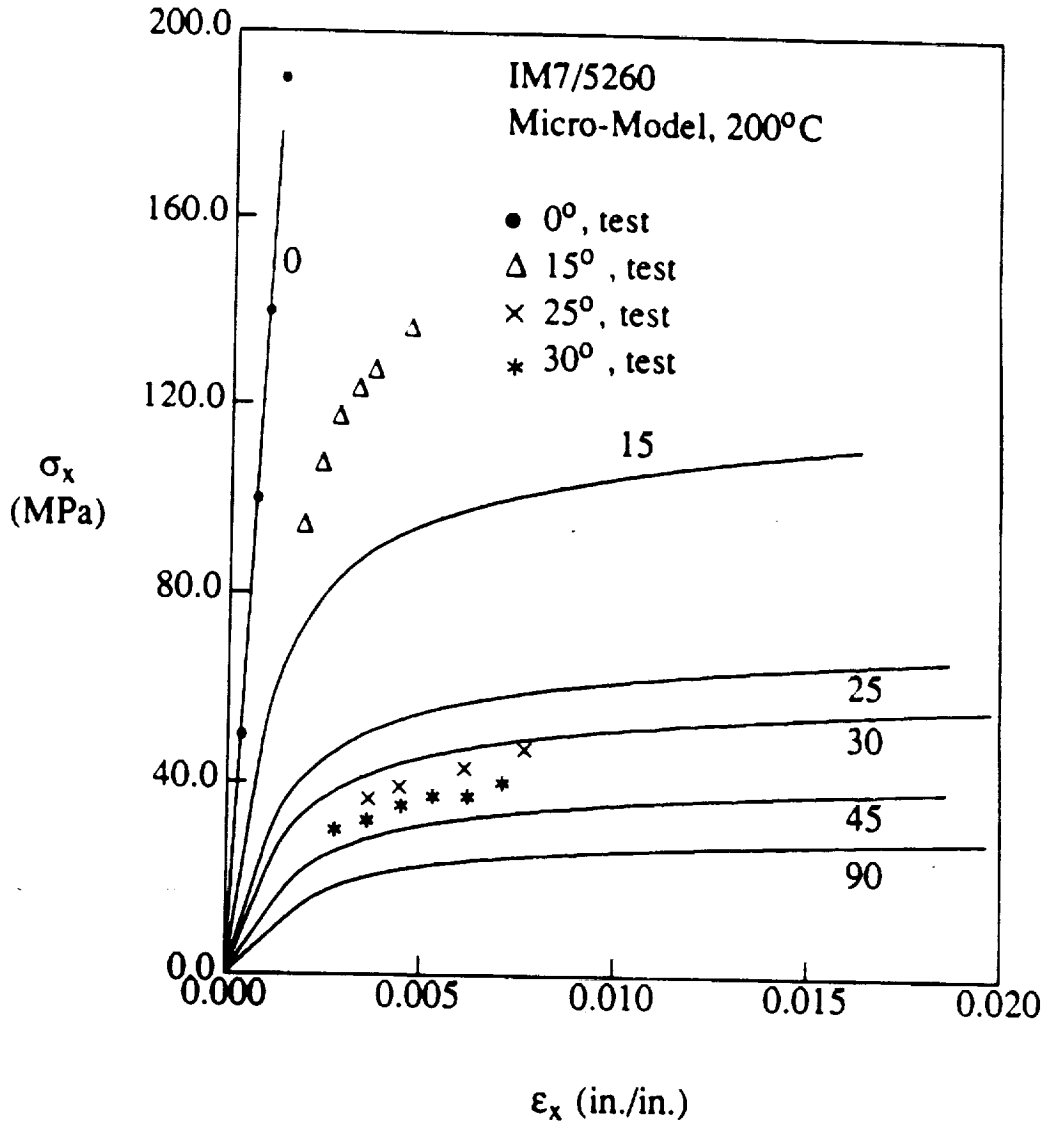

Fig. 15 Stress-strain curves for IM7/5260 at 200° C predicted by the micromechanical model. Symbols represent data from individual specimens.

REPORT DOCUMENTATION PAGE

Form Approved
OMB No. 0704-0188

1. AGENCY USE ONLY *(Leave blank)*	2. REPORT DATE	3. REPORT TYPE AND DATES COVERED
	June 1994	Technical Memorandum

4. TITLE AND SUBTITLE
Micromechanical Characterization of Nonlinear Behavior of Advanced Polymer Matrix Composites

5. FUNDING NUMBERS
WU 505-63-50-04

6. AUTHOR(S)
T. S. Gates, J. L. Chen, and C. T. Sun

7. PERFORMING ORGANIZATION NAME(S) AND ADDRESS(ES)
NASA Langley Research Center
Hampton, VA 23681-0001

8. PERFORMING ORGANIZATION REPORT NUMBER

9. SPONSORING / MONITORING AGENCY NAME(S) AND ADDRESS(ES)
National Aeronautics and Space Administration
Washington, DC 20546-0001

10. SPONSORING / MONITORING AGENCY REPORT NUMBER
NASA TM-109129

11. SUPPLEMENTARY NOTES
Gates: Langley Research Center, Hampton, VA; Chen and Sun: Purdue University, West Lafayette, IN. Presented at the ASTM 12th Symposium on Composite Materials: Testing and Design, Montreal, Canada, May 16-17, 1994.

12a. DISTRIBUTION / AVAILABILITY STATEMENT
Unclassified - Unlimited

Subject Category - 26

12b. DISTRIBUTION CODE

13. ABSTRACT *(Maximum 200 words)*

Due to the presence of curing stresses and oriented crystalline structures in the matrix of polymer matrix fiber composites, the in situ nonlinear properties of the matrix are expected to be rather different from those of the bulk resin. A plane stress micromechanical model was developed to retrieve the in situ elastic-plastic properties of Narmco 5260 and Amoco 8320 matrices from measured elastic-plastic properties of IM7/5260 and IM7/8320 advanced composites. In the micromechanical model, the fiber was assumed to be orthotropically elastic, and the matrix to be orthotropic in elastic and plastic properties. The results indicate that both in situ elastic and plastic properties of the matrices are orthotropic.

14. SUBJECT TERMS
Micromechanics; Polymer matrix composites; Temperature; Plasticity; Off-axis testing

15. NUMBER OF PAGES
38

16. PRICE CODE
A03

17. SECURITY CLASSIFICATION OF REPORT	18. SECURITY CLASSIFICATION OF THIS PAGE	19. SECURITY CLASSIFICATION OF ABSTRACT	20. LIMITATION OF ABSTRACT
Unclassified	Unclassified		